THE JOURNAL OF PHYSICAL CHEMISTRY A
A JOURNAL OF THE AMERICAN CHEMICAL SOCIETY

pubs.acs.org/JPCA Article

Laser-Induced Fluorescence Spectroscopy of Large Secondary Alkoxy Radicals: Part I. Spectral Overviews and Vibronic Analysis

Jinjun Liu* and Terry A. Miller

Cite This: *J. Phys. Chem. A* 2021, 125, 1391−1401 Read Online

ACCESS | Metrics & More | Article Recommendations | Supporting Information

ABSTRACT: We report vibronically resolved laser-induced fluorescence (LIF) spectra of jet-cooled C5−C10 secondary alkoxy radicals. The LIF spectra demonstrate vibronic structures similar to smaller (C3−C4) secondary alkoxies. For 2-pentoxy and 2-hexoxy, rotationally resolved LIF spectra have also been recorded. Two types of rotational structures have been observed in vibronic bands of each molecule. Extensive quantum chemistry calculations have been performed on 2-pentoxy and 2-hexoxy. The computed results include the relative energies of conformers, their geometries, and the energy separations between the nearly degenerate $\tilde{A}$ and $\tilde{X}$ electronic states ($\Delta E^{\tilde{A}-\tilde{X}}$). Based on the similarity between the vibronic structures of different secondary alkoxies and calculated molecular parameters, including the relative energies of conformers, the $\tilde{B} \leftarrow \tilde{X}$ transition frequencies, and the vibrational frequencies, strong vibronic bands in the LIF spectra are assigned to the origin bands and CO stretch bands of the two lowest-energy conformers of each secondary alkoxy radical. The distinct rotational structures of the two different conformations of 2-pentoxy and 2-hexoxy will be simulated and analyzed in Part II of this series (*J. Phys. Chem. A* **2021**, DOI: 10.1021/acs.jpca.0c10663).

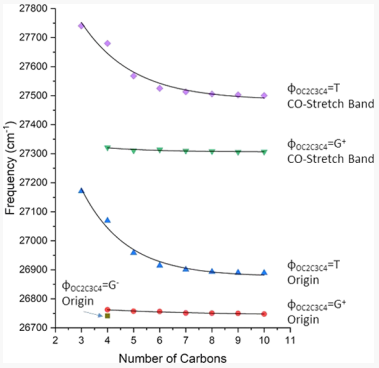

1. INTRODUCTION

Alkoxy radicals ($RO^{\bullet}$), where R stands for an alkyl group, are key reaction intermediates in the oxidation of hydrocarbons in both the combustion of fossil fuels and degradation of organic molecules in the atmosphere.[1−4] In our labs, they are studied comprehensively by laser-induced fluorescence (LIF) and dispersed fluorescence (DF) spectroscopy.[5−12] LIF spectra of both primary and secondary alkoxy radicals have been recorded with two different resolutions: the moderate-resolution spectra reveal the vibronic structure, and the high-resolution ones show the rotational and fine structures. The methoxy radical (CH_3O), the smallest alkoxy radical, is a prototypical Jahn−Teller (JT) molecule and has been subject to extensive theoretical and experimental studies.[13−17] In its ground electronic state ($\tilde{X}^2E$), CH_3O demonstrates both linear and quadratic JT effects, although its dynamic geometry on the zero-point level retains its 3-fold symmetry and still belongs to the C_{3v} point group.

For primary alkoxies other than methoxy, the degeneracy of the ^2E state is lifted, resulting in a ground $\tilde{X}$ and a low-lying $\tilde{A}$ state. The rotational and fine structures in the observed $\tilde{B} \leftarrow \tilde{X}$ high-resolution LIF spectra have been successfully simulated using the effective Hamiltonian for an asymmetric top with rotational constants for both the $\tilde{X}$ and $\tilde{B}$ states and the electron spin-rotation (SR) constants of the $\tilde{X}$ state as fit parameters.[6,18,19] Comparison between the fit rotational constants and the calculated ones, as well as analysis of the vibronic structure of the moderate-resolution spectra, enabled unambiguous assignment of the observed vibronic bands to multiple specific conformers of the primary alkoxies containing three or more carbon atoms.

The moderate-resolution (vibronically resolved) and high-resolution (rotationally resolved) LIF spectra of secondary alkoxy radicals have also been obtained in our labs. However, their analysis lagged behind that of the primary ones mainly due to the difficulty in understanding and simulating the fine structure of the high-resolution spectra. The obstacle has been overcome in recent years by implementing a newly developed "coupled-states" Hamiltonian and the use of extensive electronic structure calculations (see Part II of this series).[20] Rotational and fine structures in the high-resolution LIF spectra of isopropoxy,[21] 2-butoxy,[22,23] as well as cyclohexoxy,[24,25] have been simulated and fit, which serves as a good starting point to understanding the spectra of larger secondary alkoxies. In the present paper (called Part I), we report the moderate-resolution spectra of straight-chain secondary alkoxies with 5−10 carbon atoms. In the succeeding paper,[20] called Part II, the details of the analysis of the high-resolution spectra of 2-pentoxy and 2-hexoxy are reported. The rotational and fine structures of the high-resolution spectra of the strongest vibronic bands of 2-pentoxy and 2-hexoxy are simulated and assigned to specific conformers on the basis of the values of the molecular parameters determined. Origin and CO stretch bands in the LIF spectra

Received: November 27, 2020
Revised: January 21, 2021
Published: February 10, 2021

of these two molecules have been identified by comparing them to *ab initio* calculated $\tilde{B} \leftarrow \tilde{X}$ transition frequencies and $\tilde{B}$-state vibrational frequencies. Given these results for 2-pentoxy and 2-hexoxy, the origin and CO stretch bands in the vibronic structure of the larger secondary alkoxies (C7−C10) are also assigned based on the similarity of the vibronic structures among all secondary alkoxy radicals.

The rest of this article is organized as follows: we first briefly describe the experimental setups in Section 2. An overview of the moderate- and high-resolution LIF spectra is presented thereafter (Section 3). Quantum chemistry calculations of 2-pentoxy and 2-hexoxy are discussed in Section 4. Vibronic analysis and the conformational identifications are presented in Section 5. This article ends with a brief discussion (Section 6) and conclusions (Section 7).

2. EXPERIMENTAL SETUPS

Two experimental apparatuses were used to obtain the moderate- and high-resolution spectra of secondary alkoxy radicals, respectively, both of which were reported in detail previously.[26−29] Hence, they will be described only briefly here.

Secondary alkoxy radicals were generated in a supersonic free jet expansion by UV laser photolysis of corresponding alkyl nitrites (RONO) using a XeF excimer laser (351 nm, Lambda Physik, COMPex 110) or the third harmonics of a Nd:YAG laser (355 nm, Spectra-Physics Lasers, GCR-4). The alkyl nitrites were synthesized by the dropwise addition of concentrated sulfuric acid into a saturated solution of $NaNO_2$ and the secondary alkyl alcohols.[30] A liquid sample of the alkyl nitrites was separated and stored in a stainless steel reservoir submerged in a low-temperature bath ($T \approx -5$ °C) and was entrained in the flow by passing high-pressure helium over it. The seeded flow was then expanded through a pinhole (diameter of the orifice = 500 μm) into the vacuum chamber. The photolysis laser intercepted the jet expansion right after the orifice at the base of the nozzle.

In the moderate-resolution experiment, a dye laser (Spectra-Physics Lasers, PDL-3) pumped by the second harmonics of a Nd:YAG laser (532 nm, Spectra-Physics Lasers, GCR-4) was frequency-doubled and used to excite the $\tilde{B} \leftarrow \tilde{X}$ transition of the secondary alkoxy radicals ∼10 mm downstream. The bandwidth of the dye laser is ∼0.1 and ∼0.2 cm^{-1} after frequency-doubling. The dye laser frequency was calibrated by the optogalvanic spectra of Ne.

In the high-resolution experiment, the output of a continuous-wave (CW) ring dye laser (Coherent 899-29 Autoscan) pumped by an Ar^+ laser (Coherent Innova Sabre) was amplified in a pulsed dye amplifier (Lambda Physik, FL2003), pumped by a XeCl excimer laser (308 nm, Lambda Physik, EMG 103 MSC), frequency-doubled, and used to excite the transitions. The bandwidth of the doubled laser is ∼100 MHz. The frequency of the ring laser was calibrated by absorption spectra of iodine molecules and the transmission signal of a Fabry−Pérot etalon.

The laser-induced fluorescence was collected perpendicular to both the excitation laser beam and the jet expansion and focused through a slit onto a photomultiplier tube by two consecutive lenses. The slit was used to eliminate the fluorescence from the off-axis expansion and therefore reduce Doppler broadening. The signal was preamplified and sent to a boxcar integrator (Stanford Research Systems, SR250). The integrated signal was sent through an amplifier and recorded by a PC.

The pulse energies of the photolysis and excitation lasers were on the orders of 10 and 1 mJ, respectively. Because the laser pulse energies were not controlled stringently in the experiment, the transition intensities in both the moderate- and high-resolution LIF spectra should be regarded as quasi-quantitative. The linewidth of the moderate-resolution LIF spectra is ∼0.2 cm^{-1} dominated by the laser bandwidth, while that of the high-resolution spectra is ∼300 MHz, limited by a combination of the bandwidth of the dye amplifier and the residual Doppler broadening. The frequency accuracy of the moderate-resolution spectra is on the order of 1 cm^{-1}. The absolute frequency accuracy of the high-resolution spectra is determined by that of the iodine atlas to 0.002 cm^{-1},[31] which becomes 0.004 cm^{-1} after frequency-doubling. The relative frequency accuracy (after being doubled) is limited to about one-fifth of the spectral linewidth, i.e., ≈60 MHz.

3. SPECTRAL OVERVIEW

Moderate-resolution spectra of six secondary alkoxy radicals with 5−10 carbon atoms (2-pentoxy, 2-hexoxy, 2-heptoxy, 2-octoxy, 2-nonoxy, and 2-decoxy) in the range of ∼26 700−27 900 cm^{-1} were obtained with the vibronic structure resolved and are compared in Figure 1, together with previously reported spectra of iso-propoxy[32] and 2-butoxy.[22] For 2-pentoxy and 2-hexoxy, the spectra of the strongest vibronic bands with rotational and fine structures resolved were also obtained and are displayed in Figures 4 and 5.

3.1. Moderate-Resolution Spectra. Moderate-resolution spectra of secondary alkoxy radicals show similar patterns. All of them except iso-propoxy have the lowest-frequency strong band between ∼26 745 and ∼26 765 cm^{-1}, which is labeled "A" in Figure 1. Frequencies of the A bands of C4−C10 secondary alkoxies, determined as the frequencies of the maximum-

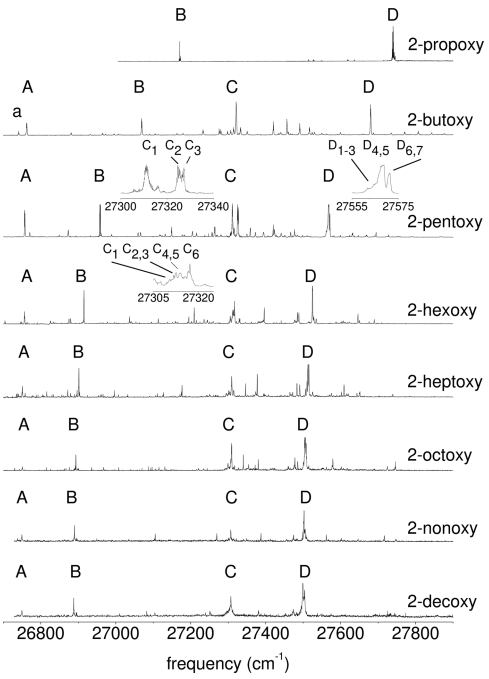

Figure 1. Moderate-resolution spectra of secondary alkoxy radicals. Spectra are adapted from ref 5. The insets show the details of split bands. See the text (Section 3) for labeling of bands. Band intensities are not quantitative due to variation in experimental conditions and the large scan range.

https://dx.doi.org/10.1021/acs.jpca.0c10662
J. Phys. Chem. A 2021, 125, 1391−1401

Table 1. Transition Frequencies of Vibronic Bands Determined as Peak Maxima in the Moderate-Resolution LIF Spectra of Secondary Alkoxy Radicals[a]

band	a	A	B	C	D
2-propoxy			27 171		27 741
2-butoxy	26 741	26 762	27 069	27 322	27 680
2-pentoxy		26 757	26 959	27 311(C_1), 27 325(C_2), 27 327(C_3)	27 568($D_{4,5}$), 27571($D_{6,7}$)
2-hexoxy		26 757	26 915	27 314(C_{1-6})	27 525
2-heptoxy		26 751	26 901	27 310	27 514
2-octoxy		26 751	26 893	27 308	27 506
2-nonoxy		26 750	26 890	27 306	27 503
2-decoxy		26 748	26 889	27 307	27 501

[a]The frequency accuracy is on the order of 1 cm^{-1}.

intensity transitions in their moderate-resolution spectra, are summarized in Table 1 and illustrated in Figure 2. It can be seen that the frequencies of Band A's decrease (red shift) slightly with an increasing number of carbon atoms. High-resolution spectra of Band A of 2-butoxy was previously obtained with rotational and fine structures resolved and was assigned to the origin of the G+ conformer, which has the clockwise *gauche*- OC2C3C4 dihedral angle. This conclusion was based on the comparison between the calculated and experimentally derived molecular parameters, particularly rotational constants.[22] Because of the localization of the half-filled (hf) electronic orbital on the O atom, the reasonable speculation is that the molecular carriers of all Band A's have the G+ OC2C3C4 structure. (See Section 4.1 for details on molecular conformations and Figure 3 for a pictorial representation of the conformers.)

The strong feature of 2-butoxy with the second-lowest frequency, labeled "B" in Figure 1, lies ~300 cm^{-1} above Band A and previously was assigned to the origin of the T conformer,[22] which has the trans OC2C3C4 dihedral angle. It is close in energy to the origin band of iso-propoxy, which is also labeled B in Figure 1. In terms of the carbon chain structure, iso-propoxy is closer to the T conformer of 2-butoxy than G+ (or G−): there is less overlap of electronic orbitals between the oxygen and the C4 carbon atom in the T conformer than in the G+ conformer, which is closer to the situation of iso-propoxy. Based on the same argument as above, the molecular carriers of all B bands in the LIF spectra of secondary alkoxies (see Figure 1) are expected to have a T structure for the OC2C3C4 dihedral angle as well. Increasing the number of carbon atoms again red-shifts the frequency of Band B, as listed in Table 1 and illustrated in Figure 2. The red shift follows roughly an exponential decay, and its magnitude is significantly larger than for Band A's.

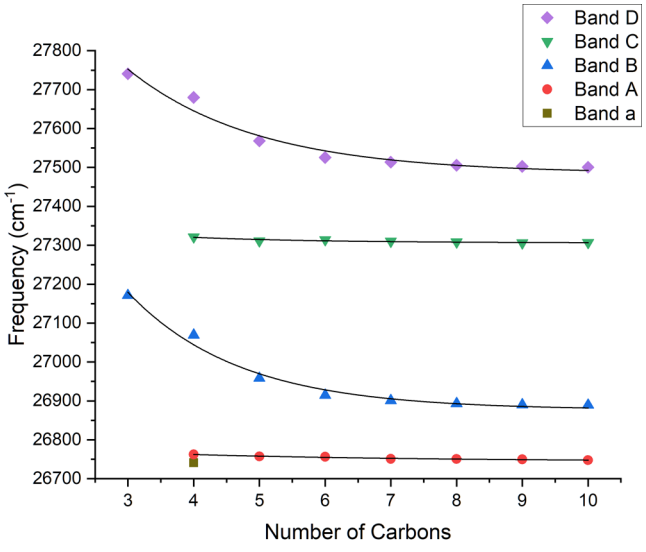

Figure 2. Transition frequencies of vibronic bands in the moderate-resolution LIF spectra of secondary alkoxy radicals as a function of the number of carbon atoms. The black curves are to guide the eye.

The CO stretch band of the G+ conformer of 2-butoxy is labeled C in Figure 1. The CO stretch bands of iso-propoxy and the T conformer of 2-butoxy are labeled D. In the spectra of larger secondary alkoxies, strong features are observed in the same region but again red-shifted. The magnitude of the red shift is significantly smaller in Bands "C" than in Band "D". The magnitudes of the red shift of Bands C are close to those of Bands A, whereas those of D close to B. As a result, the energy separations between Bands A and C are similar to those between B and D and are relatively constant between all molecules. (See Table 1 and Figure 2.) For 2-pentoxy and 2-hexoxy, Bands C and D split into multiple components. The insets in Figure 1 show the substructure of these bands on an expanded scale, with the components denoted by different subscripts.

A weak vibronic band (labeled Band "a" in Figure 1) was observed in the LIF spectrum of 2-butoxy at 36 741, ~20 cm^{-1} to the red of Band A. It was assigned to the G− conformer based on simulation of its rotational and fine structures.[22] No low-frequency vibronic bands that can be assigned to conformers with G− OC2C3C4 dihedral angles have been observed in the LIF spectra of C5−C10 secondary alkoxies presumably because of weak intensities.

3.2. High-Resolution Spectra. High-resolution spectra of Bands A, B, C, and D of 2-pentoxy and 2-hexoxy were obtained and are displayed in Figures 4 and 5, respectively. For 2-pentoxy (Figure 4), Bands A, C_1, and C_2 have similar rotational structures (hereafter referred to as "Type I"), although C_1 and C_2 have broader linewidth and, hence, more congested spectra. Bands B, C_3, and D_{1-3} have almost identical structures (hereafter referred to as "Type II"). Bands D_{1-3} partially overlap. Bands $D_{4,5}$ and $D_{6,7}$ are obviously superposition of two bands with Type II structure, which will be confirmed in Part II with spectral simulations. Based on the similarity of rotational structures, Bands A, C_1, and C_2 can be tentatively assigned to one conformer and B, C_3, and D_{1-7} to another conformer.

For 2-hexoxy, as shown in Figure 5, Bands A and C_{1-6} have similar rotation structures, which resemble those of Bands A, C_1, and C_2 of 2-pentoxy (Type I). $C_{2,3}$ and $C_{4,5}$ are overlapping bands. Bands B and D of 2-hexoxy have Type II rotational structure, the same as Bands B and D of 2-pentoxy.

The similarity in vibronic transition frequencies and rotational structures reflects the similarity between the spectral carriers,

https://dx.doi.org/10.1021/acs.jpca.0c10662
J. Phys. Chem. A 2021, 125, 1391−1401

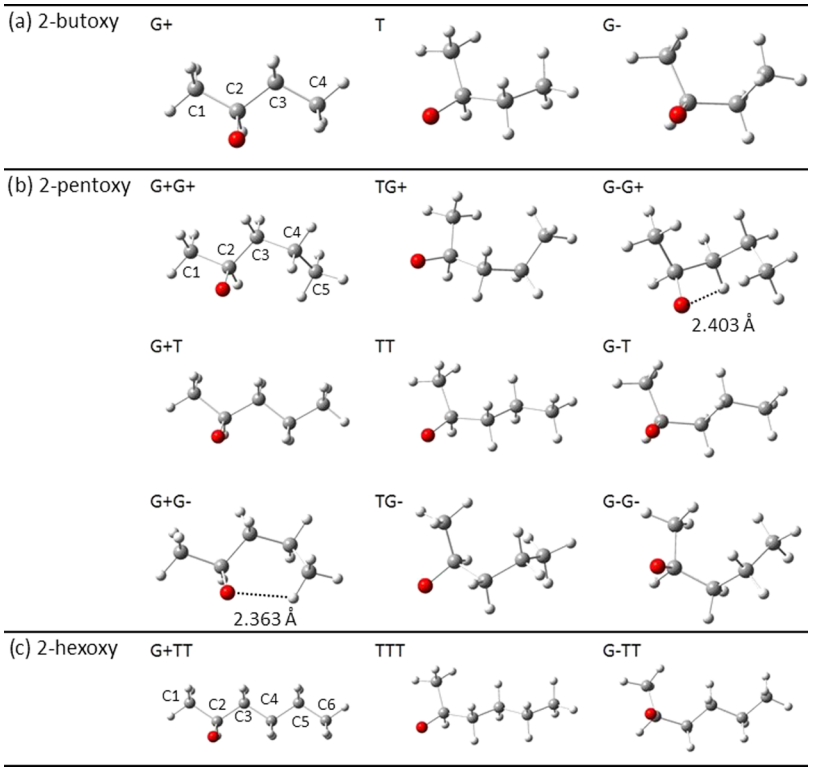

Figure 3. Structures of all three conformers of 2-butoxy, all nine conformers of 2-pentoxy, and the three lowest-energy conformers of 2-hexoxy. See the text (Section 4) for the naming of the conformers. The most important geometric parameters for 2-pentoxy and 2-hexoxy are given in Tables 2 and 3, respectively.

i.e., different conformers of the same molecule. Based on the rotational and vibrational analysis of 2-butoxy,[22] it is reasonable to speculate that the spectral carriers of vibronic bands with Type I and II rotational structures have G+ and T OC2C3C4 dihedral angles, respectively. Within each group with the same rotational structure, the lowest-frequency band is the origin band, while the bands at ~560 cm^{-1} (for Type I) or ~610 cm^{-1} (for Type II) higher frequencies are CO stretch bands. (See below.)

For the present analysis, we consider the rotational and fine structures displayed in the high-resolution spectrum only as a "fingerprint" unique to each conformer. In Part II of this series, rotational analysis and simulation of the high-resolution LIF spectra will be presented.

4. QUANTUM CHEMISTRY CALCULATIONS

The moderate-resolution LIF spectra of the secondary alkoxy radicals reveal the vibrational structure, while rotational constants and SR constants can be derived from the high-resolution LIF spectra. To support the conformational identification and vibrational assignment of different bands, as well as the simulation of the high-resolution spectra, which is presented in Part II, we performed extensive quantum chemistry calculations. All quantum chemistry calculations have been performed using the Gaussian 09 program package.[33] Various computational methods have been applied to 2-pentoxy and 2-hexoxy. The geometry optimization of the ground electronic state ($\tilde{X}$) and the first excited state ($\tilde{A}$) has been done at the B3LYP/6-31+G(d) level of theory. Different conformers have been found for each molecule by changing the dihedral angles and then optimizing the geometry. The $\tilde{A}$–$\tilde{X}$ energy separation of each conformer with and without zero-point energy (ZPE) correction has also been determined. The geometry optimization and frequency calculation of the second excited state ($\tilde{B}$) and the $\tilde{B} \leftarrow \tilde{X}$ excitation energy have been done at the CIS/6-31+G(d) level of theory. Given the relatively large size of the molecules, the Gaussian command of "Opt = loose" was used to reduce the convergence criteria to a maximum step size of 0.01 au and an RMS force of 0.0017 au.

4.1. Conformational Search and Relative Energies. For a secondary alkoxy molecule with n carbon atoms, there are $(n-3)$ C–C–C–C dihedral angles. Assuming that there are only interactions between substituents on adjacent carbon atoms, only the three completely staggered positions should be minima: *trans* (T), clockwise *gauche* (G+), and counterclockwise *gauche* (G–), "clockwise/counterclockwise" being defined as looking from the C_2 carbon to which the oxygen is attached. Because of the uniqueness of the oxygen atom, G+ and G– structures are optically distinguishable. Conformers with a reversed sequence of dihedral angles such as G+G– and G–G+ conformers of 2-pentoxy are also distinguishable. Therefore, there are 3^{n-3} conformers for a secondary alkoxy molecule with n carbon atoms. Following the convention used in our previous work on 2-butoxy,[22] conformers are labeled in the present article by the types of dihedral angles starting from OC2C3C4 (denoted by Φ_1) and then C2C3C4C5 (Φ_2), C3C4C5C6 (Φ_3), and so on. In addition, the C1C2C3C4 dihedral angle is denoted by Φ_0. The optimized geometry of all nine conformers of 2-pentoxy and the three lowest-energy conformers (out of 27) of 2-hexoxy are shown in Figure 3 in comparison to the three conformers of 2-butoxy.[22]

The relative energies of conformers of 2-pentoxy and 2-hexoxy have been calculated and are compared in Tables 2 and 3, respectively. The trends observed in the calculated results will be

https://dx.doi.org/10.1021/acs.jpca.0c10662
J. Phys. Chem. A 2021, 125, 1391–1401

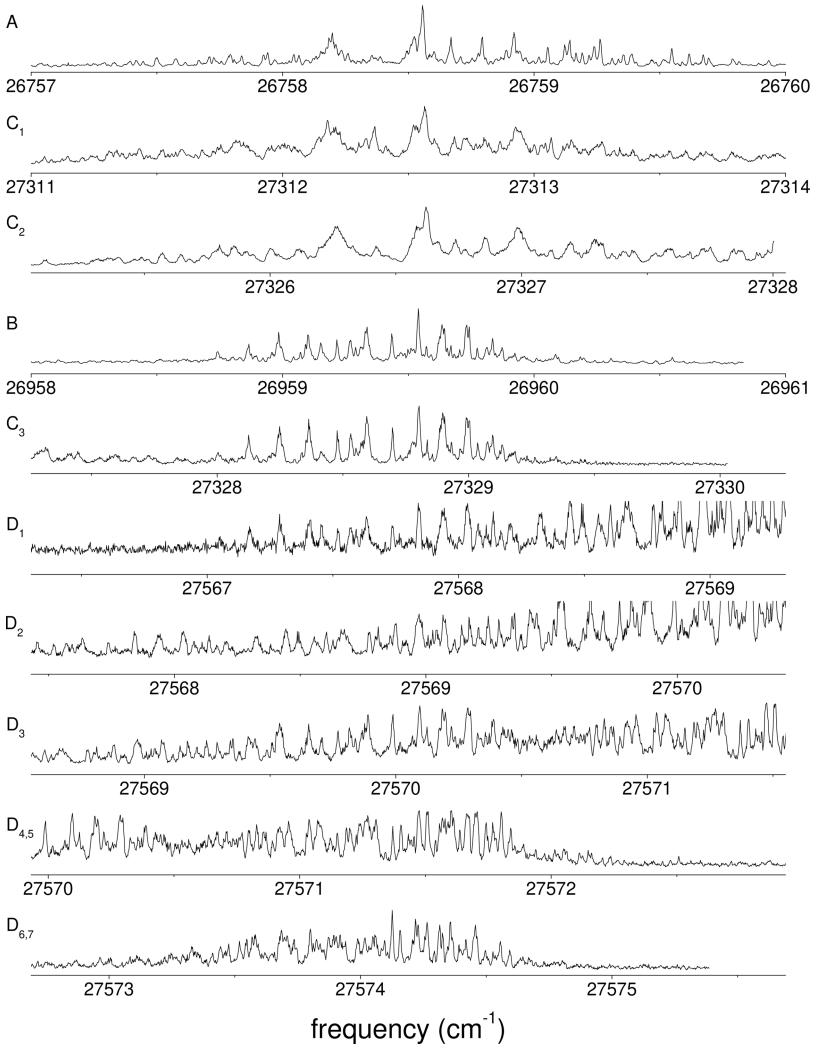

Figure 4. High-resolution spectra of different vibronic bands of 2-pentoxy.

discussed below. The relative energies of 2-pentoxy conformers without ZPE corrections (ΔE_e^{conf}) are listed in Table 2. The following observations can be made:

(i) For conformers with the same Φ_1, the one with Φ_2 = T has the lowest energy;

(ii) For the three conformers with Φ_2 =T, the relative energies of the conformers can be sorted in ascending order as Φ_1 = G+, T, G−, which is consistent with the case of 2-butoxy;[22]

(iii) For all conformers with Φ_1 = T, the energies of conformers can be sorted in ascending order as Φ_2 = T, G−, G+;

(iv) Within the three conformers with Φ_1 = G+ or G−, the conformer with Φ_1 and Φ_2 of opposite signs has the second-lowest energy, while the one with Φ_1 and Φ_2 of the same sign has the highest energy. The lower energy of the conformers with opposite-signed dihedral angles (G+G− and G−G+) is attributed to intramolecular hydrogen bonding ($R_{O...H} \sim 2.4$ Å) via a six-membered ring, as indicated in Figure 3b.

The relative energies of different conformers are so small that the inclusion of ZPEs may change the calculated energy ordering (see Table 2). Nonetheless, G+T and TT are the two lowest-energy conformers of 2-pentoxy with or without the ZPE corrections. In the previous works on primary alkoxy radicals, only the lowest-energy conformers were observed in the jet expansion. Therefore, it is reasonable to speculate that the two different rotational structures observed in the high-resolution spectra of 2-pentoxy belong to these two conformers. Such an assignment is confirmed by the rotational simulations in Part II.

For 2-hexoxy, the influence of the shape of the carbon chain for electronic energy and ZPE is more complicated than 2-pentoxy. However, the overall trends listed above for 2-pentoxy persist. For instance, for conformers with the same Φ_1, the one with $\Phi_2 = \Phi_3$= T has the lowest energy. The results for the three lowest-energy conformers (with and without the ZPE corrections), G+TT, TTT, and G−TT, are listed in Table 3. The two lowest-energy conformers are G+TT and TTT. These two conformers are presumed to be the most probable candidates for the two rotational structures observed for 2-hexoxy, which is confirmed by the rotational simulations in Part II.

4.2. $\tilde{A}$–$\tilde{X}$ Separation. In the present work, we follow the convention that the lowest-energy and the second-lowest-energy electronic states are denoted as "$\tilde{X}$" and "$\tilde{A}$", respectively. The nearly degenerate $\tilde{A}$ and $\tilde{X}$ states of primary and secondary alkoxy radicals are related to the two possible orientations of the half-filled pπ orbitals, which are largely localized on the oxygen atom in the two corresponding electron configurations:[34] the

https://dx.doi.org/10.1021/acs.jpca.0c10662
J. Phys. Chem. A 2021, 125, 1391−1401

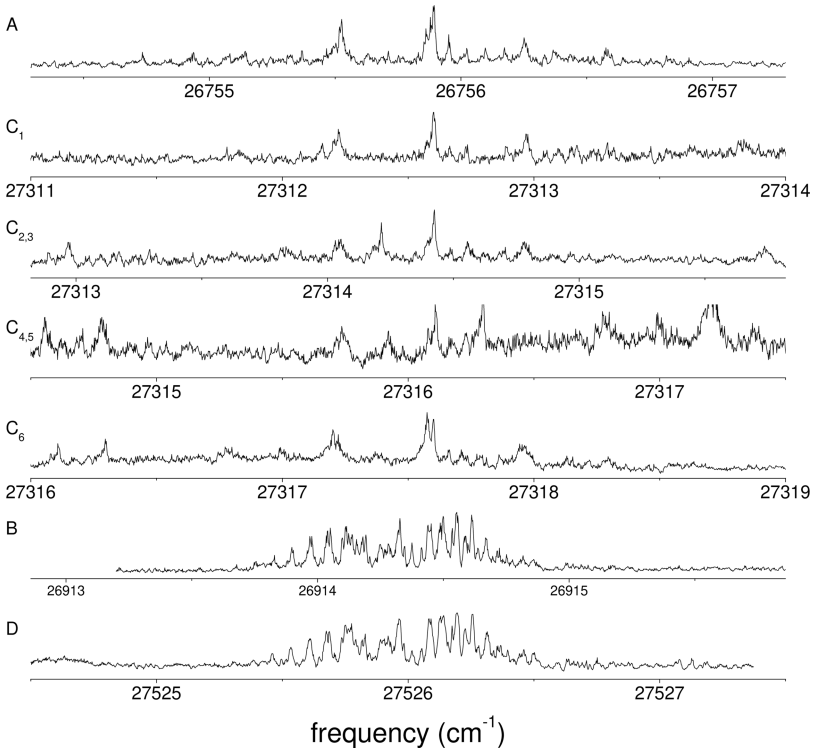

Figure 5. High-resolution spectra of different vibronic bands of 2-hexoxy.

Table 2. Calculated Relative Energies with and without ZPE Corrections of Different Conformers of 2-Pentoxy (ΔE_e^{conf} and ΔE_0^{conf}), Their $\tilde{A}-\tilde{X}$ Energy Separations with and without ZPE Corrections (ΔE_e^{ip-oop} and ΔE_0^{ip-oop}), Rotational Constants (A, B, C), Dihedral Angles (Φ's), and CO Bond Lengths (r_{CO})

conformer	ΔE_e^{conf} (cm^{-1})	ΔE_0^{conf} (cm^{-1})	hf orbital[a]	ΔE_e^{ip-oop}[b] (cm^{-1})	ΔE_0^{ip-oop}[c] (cm^{-1})	A (cm^{-1})	B (cm^{-1})	C (cm^{-1})	Φ_0[d] (deg)	Φ_1[d] (deg)	Φ_2[d] (deg)	r_{CO} (Å)
G+T	0	0	ip	−28	132	0.25428	0.05714	0.05003	−171.72	58.66	−176.90	1.3758
			oop			0.26284	0.05699	0.05039	−179.54	62.73	−179.94	1.3765
G+G−	241	328	ip	−22	31	0.22521	0.07061	0.05885	−174.29	64.83	−74.66	1.3712
			oop			0.22062	0.07233	0.05934	−173.83	68.97	−67.11	1.3764
G+G+	265	242	ip	76	248	0.20462	0.06518	0.06030	−173.52	56.77	69.26	1.3738
			oop			0.21404	0.06480	0.06031	177.59	60.04	66.45	1.3771
TT	156	238	ip	−113	95	0.23794	0.05799	0.04995	−61.60	168.86	−176.30	1.3768
			oop			0.23424	0.05939	0.05108	−64.96	172.73	−176.56	1.3732
TG−	416	402	ip	−63	175	0.18884	0.06804	0.06153	−58.93	172.33	−62.08	1.3752
			oop			0.19006	0.06873	0.06176	−60.62	176.24	−63.24	1.3723
TG+	1072	1143	ip	−54	98	0.20626	0.06788	0.05633	−59.50	170.42	93.31	1.3767
			oop			0.20264	0.06952	0.05782	−61.54	175.67	96.18	1.3733
G−T	297	328	ip	97	183	0.21562	0.06180	0.05594	65.28	−65.85	176.44	1.3755
			oop			0.22046	0.06171	0.05680	58.53	−61.56	173.08	1.3760
G−G+	489	507	ip	538	554	0.16128	0.08251	0.07341	59.79	−71.24	63.10	1.3742
			oop			0.16677	0.07872	0.07094	53.70	−66.64	69.99	1.3755
G−G−	1159	1183	ip	7	147	0.17201	0.07616	0.06424	66.43	−65.05	-87.81	1.3757
			oop			0.17913	0.07538	0.06471	58.64	−61.18	-94.98	1.3757

[a]The plane in which the half-filled (hf) orbital lies for the dominant electron configuration of the electronic state. ip = in the OCH plane, oop = perpendicular to the OCH plane. [b]Calculated energy separation between the lowest-energy and the second-lowest-energy states without the zero-point energy (ZPE) corrections. A positive (negative) sign indicates that the oop (ip) state is the ground electronic ($\tilde{X}$) state. (See the text.) [c]Calculated energy separation between the lowest-energy and the second-lowest-energy states with the zero-point energy corrections. [d]The atoms defining the dihedral angles are as follows: Φ_0 = C1C2C3C4, Φ_1 = OC2C3C4, Φ_2 = C2C3C4C5, and Φ_3 = C3C4C5C6. The eclipsed position for the alkyl chains (or O atom in Φ_1) corresponds to 0°.

half-filled pπ orbitals can either lie in the OCH plane or be perpendicular to it. Correspondingly, we also label these two nearly degenerate states according to the planes in which the half-filled pπ orbitals lie in their dominant electron configuration: "in-plane" or ip if it is in the OCH plane; "out-of-plane" or oop if it is perpendicular to the OCH plane. The small SO-free energy difference between these two states (ΔE_0) is due to the small amount of delocalization of the pπ orbitals from the O

https://dx.doi.org/10.1021/acs.jpca.0c10662
J. Phys. Chem. A 2021, 125, 1391−1401

Table 3. Calculated Results for the $\tilde{X}$ and $\tilde{A}$ States of the Three Lowest-Energy Conformers of 2-Hexoxy (of a Total of 27)[a]

conformer	ΔE_e^{conf} (cm^{-1})	ΔE_0^{conf} (cm^{-1})	hf orbital[a]	ΔE_e^{ip-oop}[b] (cm^{-1})	ΔE_0^{ip-oop}[c] (cm^{-1})	A (cm^{-1})	B (cm^{-1})	C (cm^{-1})	Φ_0[e] (deg)	Φ_1[e] (deg)	Φ_2[e] (deg)	Φ_3[e] (deg)	r_{CO} (Å)
G+TT	0	0	ip	−32	149	0.23156	0.03326	0.03060	−172.07	58.30	−176.71	−179.70	1.3756
			oop			0.23826	0.03321	0.03069	−179.69	62.60	179.78	−179.99	1.3764
TTT	267	89	ip	5	180	0.21498	0.03355	0.03054	−61.50	168.98	−175.53	−179.68	1.3768
			oop			0.22388	0.03322	0.03057	−70.32	172.33	−174.41	−179.62	1.3769
G−TT	292	171	ip	99	188	0.18064	0.03588	0.03460	64.91	−66.20	176.07	179.82	1.3754
			oop			0.18302	0.03597	0.03502	58.61	−61.56	172.19	179.27	1.3760

[a]See the title of Table 2 for meanings of notations. [b]The plane in which the half-filled (hf) orbital lies for the dominant electron configuration of the electronic state. ip = in the OCH plane, oop = perpendicular to the OCH plane. [c]Calculated energy separation between the lowest-energy and the second-lowest-energy states without the zero-point energy (ZPE) corrections. A positive (negative) sign indicates that the oop (ip) state is the ground electronic ($\tilde{X}$) state. (See the text.) [d]Calculated energy separation between the lowest-energy and the second-lowest-energy states with the zero-point energy corrections. [e]The atoms defining the dihedral angles are as follows: Φ_0 = C1C2C3C4, Φ_1 = OC2C3C4, Φ_2 = C2C3C4C5, and Φ_3 = C3C4C5C6. The eclipsed position for the alkyl chains (or O atom in Φ_1) corresponds to 0°.

Table 4. Calculated $\tilde{B}-\tilde{X}$ Energy Separations of Different Conformers of 2-Pentoxy, Their Rotational Constants (A, B, C), Dihedral Angles (Φ's), CO Bond Lengths (r_{CO}), and CO Stretch Frequencies (ν_{CO}) of the $\tilde{B}$ State

conformer	$\Delta E^{\tilde{B}-\tilde{X}}$ (cm^{-1})	A (cm^{-1})	B (cm^{-1})	C (cm^{-1})	Φ_0[a] (deg)	Φ_1[a] (deg)	Φ_2[a] (deg)	r_{CO} (Å)	ν_{CO} (cm^{-1})
G+T	28 095	0.24583	0.05826	0.05078	177.19	61.10	176.31	1.5881	742
G+G−	27 996	0.21592	0.06919	0.05784	178.82	62.47	−88.35	1.5904	733
G+G+	27 912	0.20235	0.06705	0.06151	173.32	57.27	58.73	1.5901	735
TT	28 339	0.23591	0.05788	0.04996	−71.51	172.74	−174.72	1.5880	787
TG−	28 430	0.19389	0.06593	0.05976	−68.73	175.38	−62.87	1.5889	786
TG+	28 190	0.20640	0.06726	0.05625	−70.98	173.16	92.75	1.5903	779
G−T	28 137	0.20853	0.06287	0.05709	−50.87	66.37	−176.55	1.5910	744
G−G+	28 271	0.15875	0.08006	0.07140	−43.24	74.89	−72.42	1.5902	739
G−G−	28 085	0.17362	0.07541	0.06446	−49.87	67.27	91.21	1.5922	752

[a]The atoms defining the dihedral angles are as follows: Φ_0 = C1C2C3C4, Φ_1=OC2C3C4, Φ_2 = C2C3C4C5, and Φ_3 = C3C4C5C6. The eclipsed position for the alkyl chains (or O atom in Φ_1) corresponds to 0°.

Table 5. Calculated Results for the $\tilde{B}$ States of the Three Lowest-Energy Conformers of 2-Hexoxy (of a Total of 27)[a]

conformer	$\Delta E^{\tilde{B}-\tilde{X}}$ (cm^{-1})	A (cm^{-1})	B (cm^{-1})	C (cm^{-1})	Φ_0[b] (deg)	Φ_1[b] (deg)	Φ_2[b] (deg)	Φ_3[b] (deg)	r_{CO} (Å)	ν_{CO} (cm^{-1})
G+TT	28163	0.22366	0.03384	0.03103	180	62	176	180	1.5896	737
TTT	28270	0.21585	0.03352	0.03057	−72	173	−175	−180	1.5894	786
G−TT	28133	0.17554	0.03655	0.03537	50	−67	176	180	1.5909	745

[a]See the caption of Table 4 for meanings of notations. [b]The atoms defining the dihedral angles are as follows: Φ_0 = C1C2C3C4, Φ_1= OC2C3C4, Φ_2 = C2C3C4C5, and Φ_3 = C3C4C5C6. The eclipsed position for the alkyl chains (or O atom in Φ_1) corresponds to 0°.

atom and the resulting influence from the nearby carbon and hydrogen atoms.[35] Because the $\tilde{X}$ and $\tilde{A}$ states of secondary alkoxies are almost degenerate ($\Delta E^{\tilde{A}-\tilde{X}}$ < 150 cm^{-1}), their respective dominant electron configurations, ip or oop, cannot be determined *a priori*, although they can be predicted by quantum chemistry calculations (see below) or determined in simulating high-resolution LIF spectra of the molecules (see Part II).

Previously, the $\tilde{A}-\tilde{X}$ separations and the energy ordering of the ip and oop states of ethoxy,[21] iso-propoxy,[21] and cyclohexoxy[25] were calculated using density-functional theory (DFT) methods, and the calculated values agree with experimentally determined ones quasi-quantitatively.[7] In the present work, we employed the B3LYP calculation to predict the ordering of the ip and oop states and estimate the energy separation between them. The alternation between these two states in calculations was realized by switching the β HOMO and β LUMO, both of them being pπ orbitals.[21,25]

Tables 2 and 3 list the $\tilde{A}-\tilde{X}$ separations without ZPE corrections (ΔE_e^{ip-oop}) and with ZPE corrections (ΔE_0^{ip-oop}) of the 2-pentoxy and 2-hexoxy conformers, respectively. A positive (negative) sign of ΔE_e^{ip-oop} or ΔE_0^{ip-oop} indicates that the oop (ip) state is the ground electronic ($\tilde{X}$) state, and the ip (oop) state is the first excited electronic ($\tilde{A}$) state. Also summarized in Tables 2 and 3 are the most important geometric parameters in these two electronic states, including C−C−C−C and O−C−C−C dihedral angles and CO bond lengths, and the rotational constants. Optimized geometries of all nine conformers of 2-pentoxy and the three lowest-energy conformers of 2-hexoxy in the Cartesian coordinates are given in the Supporting Information.

It has been found in calculations that, without ZPE corrections, the energy separations between the two lowest electronic states (ΔE_e^{ip-oop}) of most 2-pentoxy and 2-hexoxy conformers are less than 100 cm^{-1} (see Tables 2 and 3). When ZPE corrections are included, the energy separation (ΔE_0^{ip-oop}) can either increase or decrease, and even the energy ordering can

https://dx.doi.org/10.1021/acs.jpca.0c10662
J. Phys. Chem. A 2021, 125, 1391−1401

reverse, which is indicated by a change of sign from ΔE_e^{ip-oop} to ΔE_0^{ip-oop} (see Tables 2 and 3). With such a near-degeneracy, the question arises as to whether the quantum chemistry calculations are accurate enough to predict even the energy ordering of the two states, much less the magnitude of the $\tilde{A}-\tilde{X}$ separation. As is demonstrated in Part II, the energy ordering of those conformers with high-resolution spectra obtained can be determined experimentally by simulating the rotational and fine structures.

4.3. Second Excited State ($\tilde{B}$). The $\tilde{B}$-state geometries of both 2-pentoxy and 2-hexoxy were optimized at the CIS/6-31+G(d) level of theory. The results for all nine conformers of 2-pentoxy are listed in Table 4, and the three lowest-energy conformers of 2-hexoxy are listed in Table 5. The calculations also give the vertical $\tilde{B} \leftarrow \tilde{X}$ excitation energies. Vibrational frequencies of the $\tilde{B}$ state were calculated as well.

The second excited state of alkoxy radicals corresponds to the electronic configuration in which the half-filled orbital is oriented along the CO bond, and the $\tilde{B} \leftarrow \tilde{X}$ transition corresponds to the promotion of an electron from the pσ CO-bonding orbital to the half-filled pπ orbital on the oxygen atom. Therefore, the most significant change in geometry resulting from the transition is an increase in the CO bond length. Consequently, the most Franck−Condon-favored vibration progression is that of the CO stretch mode. The calculated $\tilde{B}$-state CO stretch frequencies of 2-pentoxy and 2-hexoxy are listed in Tables 4 and 5, respectively.

5. CONFORMATIONAL IDENTIFICATION AND VIBRONIC ANALYSIS

5.1. 2-Pentoxy. For 2-pentoxy, two distinct rotational and fine structures (Types I and II) were observed in the high-resolution LIF experiment. As discussed in Section 3, the two vibronic bands with the lowest frequencies, Bands A (with Type I structure) and B (Type II), can be tentatively assigned to the origin bands of the two lowest-energy conformers, G+T and TT, respectively, based on the similarity between the vibronic structures of 2-pentoxy and the previously studied iso-propoxy and 2-butoxy. The definitive assignment of these vibronic bands, however, requires the simulation of the rotational and fine structures of their high-resolution spectra, details of which are presented in Part II.

The rotational simulation also provides the "center" frequency (i.e., the rotationless transition frequency) of a vibronic band. Center frequencies of strong vibronic bands of 2-pentoxy are summarized in Table 6. The $\tilde{B}$-state vibrational frequencies are calculated as the relative frequencies with respect to the origin band. Comparing the vibrational frequencies to the calculated ones, Bands C and D are assigned to CO stretch bands of the G+T and TT conformers, respectively.

Band C3 has a Type II structure and belongs to TT conformer. It is unique in that it is not in the frequency region of the CO stretch but still has strong transition intensity. It is tentatively assigned to a vibration that involves the whole carbon chain. The calculated vibrational frequency is 339 cm^{-1}, compared with the experimental value of 369 cm^{-1}.

5.2. 2-Hexoxy. Given the similarity between the Type I and II bands of 2-pentoxy and 2-hexoxy, as shown in Figures 4 and 5, it is sensible to assign Type I and II bands of 2-hexoxy to the two lowest-energy conformers of 2-hexoxy, G+TT and TTT, respectively, but again confirmation is required by the simulation of the high-resolution spectra (see Part II). Center

Table 6. Absolute and Relative Frequencies of Vibronic Bands of Secondary Alkoxy Radicals[a]

molecule	band type											ν_{CO}	
												expt.[b]	calcd[c]
2-pentoxy	I	band	A		C_1	C_2							
		abs.	26758.3763		27312.3822	27326.4404							
		rel.	0		554.0059	568.0641						561.04	563.92
	II	band	B	C_3	D_1	D_2	D_3	D_4	D_5	D_6	D_7		
		abs.	26959.3272	27328.5891	27567.63	27568.86	27569.88	27571.26	27571.29	27574.02	27574.05		
		rel.	0	369.2619	608.30	609.54	610.55	611.93	611.97	614.69	614.72	611.67	598.12
2-hexoxy	I	band	A		C_1	C_2	C_3	C_4	C_5	C_6			
		abs.	26755.7053		27312.41	27314.02	27314.23	27315.92	27316.11	27317.41			
		rel.	0		556.71	558.31	558.52	560.21	560.40	561.70		559.31	560.12
	II	band	B		D								
		abs.	26914.3129		27525.9520								
		rel.	0		611.6391							611.64	597.36

[a]The absolute frequencies were determined in fitting the high-resolution LIF spectra (see Part II) with an estimated accuracy of ~0.001 cm^{-1} for separated bands. [b]Averaged values for split bands. [c]Scaled by 0.76.

https://dx.doi.org/10.1021/acs.jpca.0c10662
J. Phys. Chem. A 2021, 125, 1391−1401

frequencies of the vibronic bands and the $\tilde{B}$-state vibronic frequencies are summarized in Table 6.

5.3. Larger Secondary Alkoxies. Based on the results with 2-pentoxy and 2-hexoxy, vibronic bands in the moderate-resolution spectra of the larger secondary alkoxy radicals with 7−10 carbon atoms can be assigned with confidence even though high-resolution spectra are unavailable. Bands A and C are the origin and the CO stretch bands of the conformers with Φ_1 = G+, $\Phi_2 = \Phi_3 = ... =$ T, respectively, while Bands B and D are the origin and the CO stretch bands of the conformers with $\Phi_1 = \Phi_2 = \Phi_3 = ... =$ T, respectively.

6. DISCUSSION

6.1. Conformational Selectivity. In the supersonic expansion used in the experiments, the rotational temperatures are determined to be <2 K (see Part II). However, the initial photodissociation event producing the alkoxy radical is certainly energetic enough to produce them in any of the various conformers. Therefore, the populations and the observabilities of the given conformers will be determined by the degree of collisional cooling between the conformers leading to the lowest-energy one. This cooling will be determined by the energy available in the collisions and the barrier between the conformers.

For 2-pentoxy, G+T and TT conformers have the lowest energy with or without ZPE corrections according to the quantum chemistry calculations. It is, therefore, reasonable to assume that these conformers are the carriers of the two distinct spectra observed experimentally. Similar comments apply to the G+TT and TTT conformers and the two distinct rotational structures observed. This is consistent with facile relaxation among all of the other conformers formed, which implies rather low barriers for the process. However, the calculated energy difference (ΔE_0) between the two identified conformers is 238 cm^{-1} for 2-pentoxy. Hence, the more energetic conformer should have a negligible population if it is equilibrated at the rotational temperature. Therefore, it is reasonable to assume that the barrier between the G+T and TT 2-pentoxy conformers is sufficiently high to trap comparable numbers of conformers in the higher-energy state. Previously, the energy barrier for the T to G+ isomerization of 2-butoxy was calculated to be ∼900 cm^{-1}.[22] Calculations of the energy barriers between conformers of C5−C10 secondary alkoxies were not attempted. However, it is reasonable to assume that, for these larger alkoxies, isomerization barriers between conformers with G+ and T OC2C3C4 dihedral angles are on the same order of magnitude.

It should be said that other conformers may exist in the jet expansion since not all vibronic bands have high-resolution spectra experimentally obtained. It is unlikely, however, that their populations are comparable to those of G+T and TT conformers since all strong vibronic bands have either Type I or Type II structures. Similar conclusions can be drawn for 2-hexoxy and larger secondary alkoxy radicals. Those conformers with the G+ or T OC2C3C4 dihedral angle and the all-trans CCCC dihedral angle are the ones that are highly populated.

6.2. $\tilde{B}$−$\tilde{X}$ Electronic Transition Frequencies. The frequencies of origin bands (A's and B's) of 2-pentoxy and 2-hexoxy determined in fitting their high-resolution LIF spectra (see Part II) are listed in Table 6, while those of all secondary alkoxy radicals determined as peak maxima in their moderate-resolution spectra are listed in Table 1 and illustrated in Figure 2. (Note that the differences in vibronic transition frequencies of 2-pentoxy and 2-hexoxy in these two tables are mainly due to the significantly lower-frequency accuracy of the moderate-resolution spectra.) The origin band clearly red-shifts with the extension of the carbon chain. The $\tilde{B} \leftarrow \tilde{X}$ transition corresponds to the promotion of one electron from the CO-bonding pσ orbital to the half-filled pπ orbital localized on the O atom. The red shift is consistent with the idea that in the larger species, the longer carbon chain preferentially donates an electron directly back onto the now half-filled pσ orbital lowering the $\tilde{B}$-state energy (relative to the $\tilde{X}$ state) and strengthens the CO bond.

Comparing between the two observed conformers of a given molecule, the one with the T OC2C3C4 dihedral angle has an origin band with higher frequency, implying a stronger CO bond in the ground electronic state. The T conformers also have significantly larger red shifts for the origin bands with the extension of the carbon chain than the G+ conformers (see Figure 2) because of the stronger influence from the carbon chain. This is consistent with the calculated $\tilde{B} \leftarrow \tilde{X}$ transition frequencies. For 2-pentoxy, the difference between the calculated electronic transition frequencies of G+T and TT conformers is 244 cm^{-1}, with the former having a lower frequency. Experimentally, Band A is 201 cm^{-1} red-shifted from Band B. For 2-hexoxy, the calculated and experimental values are 107 and 159 cm^{-1}, respectively. CIS calculations usually overestimate the $\tilde{B} \leftarrow \tilde{X}$ transition frequencies of an alkoxy radical but the direction and the magnitudes of the error are similar for all conformers so that the relative transition frequencies between different conformers are better predicted.

The origin band of the G− conformer of 2-butoxy (Band a) is red-shifted from the origin band of its G+ conformer (Band A) by only ∼40 cm^{-1} because of the similarity between these two conformations. Unfortunately, no vibronic bands of other secondary alkoxy radicals with the G− OC2C3C4 dihedral angle have been observed. However, the origin bands of these conformers are expected to be close to Band A's, the origin bands of conformers with G+ OC2C3C4 dihedral angles. CIS calculations predicted that Band a of 2-pentoxy is blue-shifted from its Band A by 42 cm^{-1} (see Table 4), while Band a of 2-hexoxy is red-shifted from its Band A by 30 cm^{-1} (see Table 5).

6.3. $\tilde{B}$-State Vibrational Assignments. As with primary alkoxy radicals, given the nature of the $\tilde{B} \leftarrow \tilde{X}$ transition, the largest change in the geometries of the $\tilde{B}$ and $\tilde{X}$ states is the increase in the CO bond length (by ∼0.2 Å). The CO stretch progression, therefore, has the largest Franck−Condon factors. Comparison between the calculated CO stretch frequencies of the $\tilde{B}$ state and the experimentally determined frequency separation between Band A (B) and Band C (D) (see Table 6) further confirms the assignment of Band C (D) to the CO stretch mode of the conformer with the G+ (T) OC2C3C4 dihedral angle. A scaling factor of 0.76, however, has to be applied to match with the experimental results, which is consistent with our previous primary alkoxy,[36] iso-propoxy,[21] and 2-butoxy[22] works.

Unlike the primary alkoxy or iso-propoxy radicals, for 2-pentoxy and 2-hexoxy, as well as the larger secondary alkoxy radicals, the CO stretch region has more than one vibronic band with an almost identical structure, which either overlaps with one another or lies very close in energy. A possible mechanism, based on previous lifetime measurement of some alkoxy radicals,[37] is the internal conversion from the $\tilde{B}$ state to the semicontinuum of $\tilde{X}$- or $\tilde{A}$-state vibrational levels at this energy. More theoretical and computational work is required for a more

https://dx.doi.org/10.1021/acs.jpca.0c10662
J. Phys. Chem. A 2021, 125, 1391−1401

quantitative explanation to the splitting, which is beyond the scope of the present paper.

7. CONCLUSIONS

We have recorded the moderate-resolution $\tilde{B} \leftarrow \tilde{X}$ LIF spectra of 2-alkoxy radicals with 5−10 carbons under the jet-cooled conditions, which reveal the vibronic structures of these molecules. High-resolution spectra with the resolved rotational and fine structures of the smallest two, 2-pentoxy and 2-hexoxy, have also been obtained. For each of these two molecules, two types of rotational structures have been observed, suggesting two molecular carriers. By comparing the calculated and experimentally determined $\tilde{B}-\tilde{X}$ transition frequencies and $\tilde{B}$-state vibrational frequencies, the strongest vibronic bands in the spectra of 2-pentoxy and 2-hexoxy are assigned to the origin bands and CO stretch bands of their two lowest-energy conformers. Vibronic structures of the larger secondary alkoxies can also be assigned based on the similarity between the moderate-resolution LIF spectra of all of the molecules.

■ ASSOCIATED CONTENT

Supporting Information

The Supporting Information is available free of charge at https://pubs.acs.org/doi/10.1021/acs.jpca.0c10662.

Cartesian coordinates of optimized geometries of 2-pentoxy and 2-hexoxy conformers (PDF)

■ AUTHOR INFORMATION

Corresponding Author

Jinjun Liu − *Department of Chemistry, University of Louisville, Louisville, Kentucky 40292, United States; Department of Physics, University of Louisville, Louisville, Kentucky 40292, United States;* orcid.org/0000-0002-3968-2059; Email: j.liu@louisville.edu

Author

Terry A. Miller − *Department of Chemistry, The Ohio State University, Columbus, Ohio 43210, United States;* orcid.org/0000-0003-0731-8006

Complete contact information is available at: https://pubs.acs.org/10.1021/acs.jpca.0c10662

Notes

The authors declare no competing financial interest.

■ ACKNOWLEDGMENTS

The authors are grateful to Drs. Christopher C. Carter and Sandhya Gopalakrishnan for taking the LIF spectra. This work was supported by the National Science Foundation under Grant Nos. CHE-1454825 and CHE-1955310. T.A.M. acknowledges support from the Ohio Supercomputer *via* Project No. PAS0540.

■ REFERENCES

(1) Ghigo, G.; Maranzana, A.; Tonachini, G. Combustion and Atmospheric Oxidation of Hydrocarbons: Theoretical Study of the Methyl Peroxyl Self-Reaction. *J. Chem. Phys.* **2003**, *118*, 10575.

(2) Compton, R. G.; Hancock, G. *Chemical Kinetics*; Elsevier: Amsterdam, 1997.

(3) Finlayson-Pitts, B. J.; Pitts, J. J. N. *Chemistry of the Upper and Lower Atmosphere*, 3rd ed.; Academic: New York, 2000; Chapter 6.

(4) Curran, H. J.; Gaffuri, P.; Pitz, W. J.; Westbrook, C. K. A Comprehensive Modeling Study of *n*-Heptane Oxidation. *Combust. Flame* **1998**, *114*, 149.

(5) Carter, C. C.; Gopalakrishnan, S.; Atwell, J.; Miller, T. A. Laser Excitation Spectra of Large Alkoxy Radicals Containing 5 to 12 Carbon Atoms. *J. Phys. Chem. A* **2001**, *105*, 2925.

(6) Zu, L.; Liu, J.; Gopalakrishnan, S.; Miller, T. A. The Rotationally Resolved Electronic Spectra of Several Conformers of 1-Hexoxy and 1-Heptoxy. *Can. J. Chem.* **2004**, *82*, 854.

(7) Jin, J.; Sioutis, I.; Tarczay, G.; Gopalakrishnan, S.; Bezant, A.; Miller, T. A. Dispersed Fluorescence Spectroscopy of Primary and Secondary Alkoxy Radicals. *J. Chem. Phys.* **2004**, *121*, 11780.

(8) Alam, J.; Reza, M. A.; Mason, A.; Reilly, N. J.; Liu, J. Dispersed Fluorescence Spectroscopy of Jet-Cooled 2-, 3-, and 4-Methylcyclohexoxy Radicals. *J. Phys. Chem. A* **2015**, *119*, 6257−6268.

(9) Liu, J.; Reilly, N. J.; Mason, A.; Miller, T. A. Laser-Induced Fluorescence Spectroscopy of Jet-Cooled t-Butoxy. *J. Phys. Chem. A* **2015**, *119*, 11804−11812.

(10) Reza, M. A.; Paul, A. C.; Reilly, N. J.; Alam, J.; Liu, J. Dispersed Fluorescence Spectroscopy of Jet-Cooled Isobutoxy and 2-Methyl-1-butoxy Radicals. *J. Phys. Chem. A* **2016**, *120*, 6761−6767.

(11) Reza, M. A.; Paul, A. C.; Reilly, N. J.; Liu, J. Laser-Induced Fluorescence and Dispersed Fluorescence Spectroscopy of Jet-Cooled Isopentoxy Radicals. *J. Phys. Chem. A* **2019**, *123*, 8441−8447.

(12) Koncz, B.; Bazsó, G.; Reza, M. A.; Telfah, H.; Heged us, K.; Liu, J.; Tarczay, G. Revealing Long-Range Substituent Effects in the Laser-Induced Fluorescence and Dispersed Fluorescence Spectra of Jet-Cooled $CH_xF_{3-x}CH_2O$ (x = 1, 2, 3) Radicals. *J. Phys. Chem. A* **2019**, *123*, 10947−10960.

(13) Hougen, J. T. Double Group Considerations, Jahn-Teller Induced Rovibronic Effects, and the Nuclear Spin-Electron Spin Hyperine Hamiltonian for a Molecule of Symmetry C_{3v} in an Electronic ^{2}E State. *J. Mol. Spectrosc.* **1980**, *81*, 73.

(14) Watson, J. K. G. Jahn-Teller and L-Uncoupling Effects on Rotational Energy Levels of Symmetric and Spherical Top Molecules. *J. Mol. Spectrosc.* **1984**, *103*, 125.

(15) Endo, Y.; Saito, S.; Hirota, E. The Microwave Spectrum of the Methoxy Radical CH_3O. *J. Chem. Phys.* **1984**, *81*, 122.

(16) Liu, J.; Chen, M.-W.; Melnik, D.; Yi, J. T.; Miller, T. A. The Spectroscopic Characterization of the Methoxy Radical (Part I): Rotationally Resolved $\tilde{A}^2A_1-\tilde{X}^2E$ Electronic Spectra of CH_3O. *J. Chem. Phys.* **2009**, *130*, No. 074302.

(17) Liu, J.; Chen, M.-W.; Melnik, D.; Miller, T. A.; Endo, Y.; Hirota, E. The Spectroscopic Characterization of the Methoxy Radical (Part II): Rotationally Resolved $\tilde{A}^2A_1-\tilde{X}^2E$ Electronic and $\tilde{X}^2E$ Microwave Spectra of the Perdeuteromethoxy Radical CD_3O. *J. Chem. Phys.* **2009**, *130*, No. 074303.

(18) Gopalakrishnan, S.; Carter, C. C.; Zu, L.; Stakhursky, V.; Tarczay, G.; Miller, T. A. Rotationally Resolved $\tilde{B}-\tilde{X}$ Electronic Spectra of Both Conformers of the 1-Propoxy Radical. *J. Chem. Phys.* **2003**, *118*, 4954.

(19) Gopalakrishnan, S.; Zu, L.; Miller, T. A. Rotationally Resolved Electronic Spectra of the $\tilde{B}-\tilde{X}$ Transition in Multiple Conformers of 1-Butoxy and 1-Pentoxy Radicals. *J. Phys. Chem. A* **2003**, *107*, 5189.

(20) Liu, J.; Chen, M.-W.; Miller, T. A. Laser-Induced Fluorescence Spectroscopy of Large Secondary Alkoxy Radicals. Part II. Rotational and Fine Structure. *J. Phys. Chem. A* **2021**, DOI: 10.1021/acs.jpca.0c10663.

(21) Liu, J.; Melnik, D.; Miller, T. A. Rotationally Resolved $\tilde{B} \leftarrow \tilde{X}$ Electronic Spectra of the Isopropoxy Radical: A Comparative Study. *J. Chem. Phys.* **2013**, *139*, No. 094308.

(22) Stakhursky, V.; Zu, L.; Liu, J.; Miller, T. A. High-Resolution Spectra and Conformational Analysis of the 2-Butoxy Radical. *J. Chem. Phys.* **2006**, *125*, No. 094316.

(23) Yan, Y.; Sharma, K.; Miller, T. A.; Liu, J. Rotational and Fine Structure of Open-Shell Molecules in Nearly Degenerate Electronic States. II. Interpretation of Experimentally Determined Interstate Coupling Parameters of Alkoxy Radicals. *J. Chem. Phys.* **2020**, *153*, No. 174306.

(24) Zu, L.; Liu, J.; Tarczay, G.; Dupre, P.; Miller, T. A. Jet-Cooled Laser Spectroscopy of the Cyclohexoxy Radical. *J. Chem. Phys.* **2004**, *120*, 10579.
(25) Liu, J.; Miller, T. A. Jet-Cooled Laser-Induced Fluorescence Spectroscopy of Cyclohexoxy: Rotational and Fine Structure of Molecules in Nearly Degenerate Electronic States. *J. Phys. Chem. A* **2014**, *118*, 11871.
(26) Foster, S. C.; Miller, T. A. The Spectroscopy of Transient Species in Supersonic Free Jet Expansions. In *Laser Applications in Physical Chemistry*; Marcel Dekker, Inc.: New York, NY, 1989; p 307.
(27) Foster, S. C.; Kennedy, R. A.; Miller, T. A. Laser Spectroscopy of Chemical Intermediates in Supersonic Free Jet Expansions. In *NATO ASI Series, Frontiers of Laser Spectroscopy of Gases*; Alves, A. C. P.; Brown, J. M.; Hollas, J. M., Eds.; Kluwer Academic Publishers: Dordrecht, 1988; p 421.
(28) Liu, X.; Foster, S. C.; Williamson, J. M.; Yu, L.; Miller, T. A. The Spin-Rotation Interactions in the Methoxy Radical. *Mol. Phys.* **1990**, *69*, 357.
(29) Tan, X.-Q.; Wright, T. G.; Miller, T. A. Electronic Spectroscopy of Free Radicals in Supersonic Jets. In *Jet Spectroscopy and Molecular Dynamics*; Hollas, J. M.; Phillips, D., Eds.; Blackie Academic: London, 1995; p 74.
(30) Blatt, A. H. *Organic Synthesis II*; Wiley: New York, 1963.
(31) Gerstenkorn, S.; Vergès, J.; Chevillard, J. *Atlas du Spectre d'Absorption de la Molécule d'Iode: 11000-14000 cm^{-1}*; Laboratoire Aimé-Cotton CNRS II: Orsay, 1982.
(32) Chhantyal-Pun, R.; Roudjane, M.; Melnik, D. G.; Miller, T. A.; Liu, J. Jet-Cooled Laser-Induced Fluorescence Spectroscopy of Isopropoxy Radical: Vibronic Analysis of $\tilde{B} - \tilde{X}$ and $\tilde{B} - \tilde{A}$ Band Systems. *J. Phys. Chem. A* **2014**, *118*, 11852.
(33) Frisch, M. J.; et al. *Gaussian 09*, revision A.1; Gaussian Inc.: Wallingford, CT, 2009.
(34) Foster, S. C.; Hsu, Y.-C.; Damo, C. P.; Liu, X.; Kung, C.-Y.; Miller, T. A. The Implications of the Rotationally Resolved Spectra of the Alkoxy Radicals for Their Electronic Structure. *J. Phys. Chem. A* **1986**, *90*, 6766.
(35) Mills, P. D. A.; Western, C. M.; Howard, B. J. Rotational Spectra of Rare Gas-Nitric Oxide van der Waals Molecules. Part 1. Theory of the Rotational Energy Levels. *J. Phys. Chem. A* **1986**, *90*, 3331−3338.
(36) Tarczay, G.; Gopalakrishnan, S.; Miller, T. A. Theoretical Prediction of Spectroscopic Constants of 1-Alkoxy Radicals. *J. Mol. Spectrosc.* **2003**, *220*, 276.
(37) Gopalakrishnan, S.; Zu, L.; Miller, T. A. Radiative and Non-Radiative Decay of Selected Vibronic Levels of the $\tilde{B}$ State of Alkoxy Radicals. *Chem. Phys. Lett.* **2003**, *380*, 749.

https://dx.doi.org/10.1021/acs.jpca.0c10662
J. Phys. Chem. A 2021, 125, 1391−1401